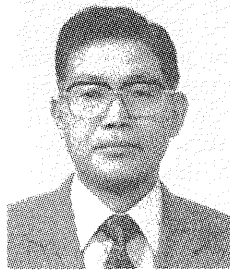


EVALUATION OF EARTHQUAKE-DAMAGED RC PIERS BY
THE ULTIMATE BEARING CAPACITY PROCEDURE

(Translation from Proceeding of JSCE, No. 592/V-39, May 1998)



Kenji KOSA



Manabu FUJII



Hidenao HAYASHI



Tsunekazu NAKATA

To formulate design concepts for seismic retrofitting, a detailed damage investigation was conducted on RC single piers along the Hanshin Expressway Kobe Route, which was severely damaged by the 1995 Hanshin Awaji Earthquake. Using the data obtained, the relationship between damage level and ultimate bearing capacity required by the Specifications for Highway Bridges of 1990 was evaluated quantitatively.

According to the results, a considerable correlation was found between damage level and the shear strength of the piers. Namely, severely damaged piers tended to have small values of shear strength vs. flexural strength ratio as well as of shear strength index.

Keywords: ductility, failure mechanism, shear, flexure, earthquake resistance

Kenji Kosa, a member of the JSCE and ASCE, is an associate professor in the Department of Civil Engineering at the Kyushu Institute of Technology. Before joining the faculty in 1999, he was a senior highway engineer at the Hanshin Expressway Public Corporation. He obtained his Ph.D. from the University of Michigan in 1988. His main research interests are the design and analysis of concrete structures.

Manabu Fujii was a professor in the Department of Civil Engineering at Kyoto University. After 35 years of professorship at both Kobe and Kyoto Universities and leaving several books and numerous papers in the fields of prestressed concrete and reinforced concrete, the distinguished professor passed away of illness in 1997.

Hidenao Hayashi is a director of the Research and Development Division at the Hanshin Expressway Management Technology Center. He obtained his Dr. Eng. from Osaka University in 1998. He worked for the restoration of the Hanshin Expressway Kobe Route during 1995 and 1997. His research interest is the design of steel and concrete structures. He is a fellow member of the JSCE.

Tsunekazu Nakata is a section manager at Yachiyo Engineering Co., Ltd. He obtained his MS in civil engineering from Kyoto University in 1977. His research interest is the seismic design of concrete structures. He is a registered consulting engineer and a member of the JSCE.

1. INTRODUCTION

The Hanshin Awaji Earthquake of 1995 caused tremendous damage to the bridge structures of the Hanshin Expressway. Damage was especially disastrous along the Kobe Route, where girders fell to the ground and piers collapsed. The immediate cause of this devastation was said to be the overwhelming intensity of seismic forces. Aside from this overriding cause, insufficient shear strength, inadequate anchoring length of main reinforcement at its termination point, and lack of ductility were indicated as the structural causes [1]. Immediately after the earthquake, all RC piers along the Kobe Route were inspected visually to identify their degree of damage as the first-round inspection. Piers assessed as severely damaged were dismantled for reconstruction and those found to have relatively light damage were to be repaired or strengthened. Piers designated for repair or strengthening were checked again for degree of damage, including the situation under the ground, to determine the details of retrofit design such as the range for replacing reinforcement or repairing the concrete.

Inspection of bridges and buildings for post-earthquake damage has been carried out many times in Japan, where earthquakes are a part of our history. However, they have mostly been performed by visual methods only, and results have almost never been compared with the results of detailed damage investigations. Similarly, reports of numerical analysis targeting individual structures are many, but it is quite rare for a number of identical structures, such as RC single piers, to be checked for ultimate lateral strength as a group [2] ~ [4].

In the present study, a quantitative evaluation was first carried out on the damage to RC single piers along the Kobe Route. Then, macroscopic damage analysis was performed to find the relationship between strength and degree of damage by conducting an ultimate lateral strength check according to the procedure in the Specifications for Highway Bridges of 1990 (Highway Specifications).

2. STRUCTURES ALONG THE KOBE ROUTE

Most of the bridge piers along the severely damaged 27.7 km section on the Kobe Route that runs through the area affected by a JMA intensity of 7 or greater were constructed in the late 1960s based on the Highway Specifications for Steel Bridges of 1964. Many of the piers were of the RC single column type because the route, elevated all the way, runs directly above space-restricted National Roads 2 and 43. The ground is mostly of II type consisting of sand and gravel layers. Of the foundations, 84% are pile foundations and 12% spread foundations. Of the bridge girders, 86% are steel with a breakdown of 80% simple I girders, 10% simple box girders, 5% continuous I girders, and 5% continuous box girders. The design horizontal seismic coefficient at the time of construction was 0.2. The allowable shear stress for concrete was 7 kgf/cm², which was considerably greater than the 4.2 kgf/cm² specified in the standards of 1971. In those days, it was commonly considered that the concrete cross section was enough to provide sufficient shear strength. As a result, hoop ties formed by D16 reinforcing bars were placed at a spacing of 15 ~ 30 cm.

In the damage inspection carried out immediately after the earthquake, piers were assessed into five damage ranks from As (most severe) through A, B, and C, to D (minor or no damage) according to the assessment procedure given in the Manual for Earthquake Disaster Countermeasures for Highway Bridges: Post-Earthquake Countermeasures [5]. The results of this inspection are shown in Table 1. Of the 943 piers in the severely affected 27.7 km section, 15% were ranked As and A, and 35% B and C [6]. Piers ranked As and A were to be reconstructed, and those given B, C, and D ranks were assessed for repair or strengthening. Foundations were all reused because they were found to be virtually unaffected by the earthquake, though slight cracking was observed on piles.

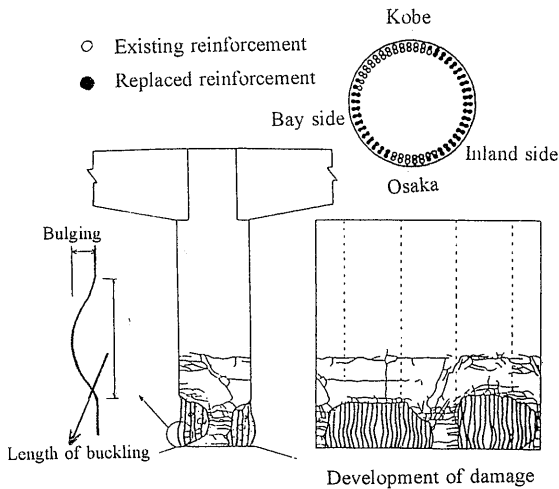


Fig.1 Development of damage

Table 1 Number of piers with each damage level

	As	A	B	C	D	Total
Steel piers	3	8	12	112	28	163
RC piers	64	78	102	225	474	943
Total	67	86	114	337	502	1106

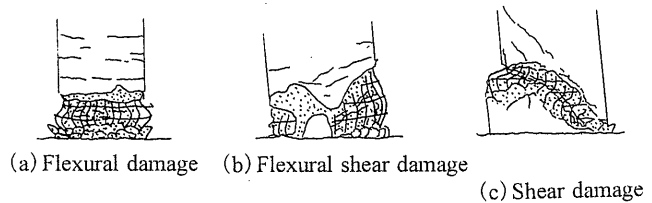


Fig.2 Damage types

3. DETAILED DAMAGE ASSESSMENT

3.1 Detailed investigation

All the piers ranked B, C, and D in the first-round visual inspection were reinvestigated, including an investigation of damage situation below ground, so as to determine the details of retrofit design. Piers of As and A ranks were not investigated because some had already been enclosed in steel plates in emergency safety operations and others were too dangerous for investigators to approach.

First, figures showing the actual damages to concrete and reinforcement were prepared, as given in Fig. 1. With regard to the concrete, the range over which the cover concrete had fallen away, the size of cracks, and their distribution were measured. As to the reinforcement, the buckling length of main reinforcement and the amount of bulge were measured. All 818 piers along the severely affected 27.7 km section, excluding ramp piers, were reinvestigated.

3.1.1 Detailed damage ranking

Piers of ranks As and A were not reinvestigated for the reason given above. Therefore, their previously-determined As and A ranks were used as they were. Piers of rank B and C were grouped into sub-categories based on the reinvestigation results. Namely, rank B was divided into B1, B2, and B3 according to the proportion of main reinforcement requiring replacement and rank C into C1 and C2 based on the degree of damage to the concrete. Rank D was not divided because there was no utility grouping piers that need neither repair nor strengthening.

As: piers collapsed or nearly collapsed

A: conspicuous buckling of the main reinforcement observed around the entire circumference of

the column

B1: main reinforcement needs replacement because of bulging around the entire circumference of the column

B2: about 1/2 of main reinforcement needs replacement

B3: about 1/4 of main reinforcement needs replacement

C1: part of main reinforcement exposed, but no bulging of main reinforcement

C2: main reinforcement not exposed, but major cracks observed

D: minor cracks or no damage observed

3.1.2 Grouping by damage type

Pier damage was grouped into three types based on the results of the original visual inspection and the detailed investigation: shear damage, flexural damage, and flexural shear damage. The type of damage was determined according to the descriptions in Fig. 2 and the definitions given below. This process of categorization was not easy because some piers were too severely damaged to assess and others had suffered evolving types of damage as the earthquake progressed.

① Shear damage: primary cracking angle or angle of damaged plane is diagonal to the cross section. Concrete is severely damaged, and in some cases, a large gap is observed between upper and lower members on the damage plane.

② Flexural damage: in piers with little damage, the primary cracking angle is lateral, while in the piers with major damage, the main reinforcement is buckled outward.

③ Flexural shear damage: this damage type is difficult to assess, but piers in-between shear damage and flexural damage were simply categorized as this type. Accordingly, even though the main reinforcement buckled outward over the entire circumference of a pier, if the buckling occurred diagonal to the cross section or was unbalanced to the left and right sides, it was regarded as of the flexural shear type.

3.2 Evaluation of strength

Using the check method for ultimate lateral strength prescribed in the Highway Specifications of 1990, the ultimate bearing capacity of the RC single piers that are dominant in number and relatively severely damaged among the RC piers on the Kobe Route was evaluated. The four equations used for evaluation are given below.

$$\lambda = \nu \cdot S_u \cdot l_a / (M_u - M_o) \dots\dots\dots (1)$$

where

λ : shear strength vs. flexural strength ratio

ν : safety factor (1.0 was used for analysis)

S_u : shear strength (tf)

l_a : distance from cross section of interest to the point at which inertial force was imposed from the superstructure (m).

M_u : bending moment at the time compressive strain on the outermost layer of concrete reaches the ultimate strain on the plane to which a uniform axial force is imposed. (tf · m)

M_o : eccentric moment in the direction perpendicular to the bridge axis (tf · m)

$$\begin{aligned} \alpha_{su} &= 980 \cdot S_u / (W_u + W_p) \\ \beta_{su} &= \alpha_{su} / 200 \dots\dots\dots (2) \end{aligned}$$

where

α_{su} : shear strength index (gal)

W_u : weight of the superstructure carried by pier (tf)

W_p : weight of pier (tf)

β_{su} : safety factor for shear strength

$$\begin{aligned} \alpha_{my} &= 980 (M_y - M_o) / (W_u + 0.5 W_p) \cdot l_a \\ \beta_{my} &= \alpha_{my} / 200 \dots\dots\dots (3) \end{aligned}$$

where

α_{my} : yield flexural strength index (gal)

M_y : bending moment at the time the tensile reinforcement on the outermost layer reaches the yield stress at the cross section to which a uniform axial force is imposed (tf · m)

β_{my} : safety factor for flexural strength

$$\begin{aligned} \alpha_{mu} &= \alpha_{my} \cdot \sqrt{2\mu - 1} \\ \beta_{mu} &= \alpha_{mu} / 200 \\ \mu &= \delta u / \delta y \end{aligned} \quad (4)$$

where

α_{mu} : ultimate flexural strength index (gal)

β_{mu} : safety factor for ultimate flexural strength

μ : ductility factor

δu : ultimate flexural displacement (m)

δy : yield flexural displacement (m)

Damage analysis was conducted according to the flowchart in Fig. 3. Though the shear strength of a pier (S_u) was calculated based on the procedure given in the Highway Specifications, it was also compared with the shear strength obtained from the procedure in the Standard Specifications for Concrete (Concrete Specifications) [7] [8]. In both procedures, the shear strength was calculated by adding the shear strength carried by the concrete and that carried by the reinforcement, but when it came to the calculation of the average shear stress of the concrete, the procedure in the Concrete Specifications takes into account the effects of the size of the member and the quantity of main reinforcement.

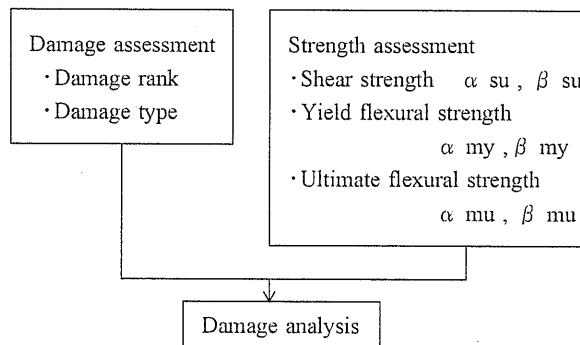


Fig.3 Flowchart of checking process

The shear strength index (α_{su}) is obtained by dividing the shear strength of a member by the weight of the structure, and it indicates an acceleration (gal) equivalent to the shear strength. The safety factor for shear strength (β_{su}) is obtained by dividing the shear strength index by an acceleration (200 gal) equivalent to the design seismic coefficient used in the original design. The flexural strength and ductility factor were calculated from the Retrofit Specifications [9] [10]. In these Retrofit Specifications, the confinement effect of hoop ties is taken into account in the stress-strain curve of concrete and, therefore, both the curve and the ultimate strain will change according to the amount of confining reinforcement.

The yield flexural strength index (α_{my}) represents the acceleration that causes a bending moment large enough to make the main reinforcement on the outer-most layer reach the yield stress ($\sigma_{sy} = 3000 \text{ kgf/cm}^2$) under a uniform axial stress. A safety factor for yield flexural strength (β_{my}) is obtained by dividing the yield flexural strength index by an acceleration (200 gal) equivalent to the design seismic coefficient of the original design. Presupposing the energy conservation law, the ultimate flexural strength index (α_{mu}) represents the elastic acceleration that causes an ultimate displacement (δu) in the elasto-plastic model. A safety factor for ultimate flexural strength (β_{mu}) is obtained by dividing α_{mu} by 200 gal, as with β_{my} .

4. EVALUATION OF DAMAGE

4.1 Damage type and damage level

Of the 818 piers along the severely affected 27.7 km section (excluding the ramp piers), RC single piers accounted for 67.7% (553 piers). As to cross section, 70.7% (391 piers) were circular and 29.3% (162 piers) rectangular (including oval designs). Figure 4 shows the ratio of the three damage types for RC single piers at all damage levels. These ratios reflect results for 428 piers, because some had been removed because of serious damage and replaced. Figure 5 shows similar ratios but focusing only on piers with relatively severe damage, or those ranked As, A, B1, B2, and B3. In Fig. 4, flexural damage accounts for 54.0%, flexural shear damage 41.4%, and only the remaining 4.7% was shear damage. In contrast, in Fig. 5 where the focus is piers with relatively severe damage, the proportion of shear damage and flexural shear damage is substantially increased while the ratio of flexural damage is proportionally lowered.

The distribution of flexural damage is very wide - A: 7.8%, B: 20.4%, C: 61.9%, and D: 10.0%. This is probably because, in the case of flexural damage, no abrupt fracture occurs because energy absorption continues even after plasticization takes place. Much of the damage is relatively light and at the flexural yielding level before it progresses to more severe flexural shear damage. The distribution of shear damage and flexural shear damage is As and A: 61.4%, B: 17.3%, C: 17.8%, and D: 3.6%. As seen, most corresponds to relatively severe damage at levels As, A, and B. The reason for this is that shear damage rarely stops at the level of light damage because this type of damage progresses quite fast.

4.2 Comparison of results

Figure 6 compares the damage levels obtained from visual inspections and detailed investigations. Here, piers ranked B, C, and D by visual inspection are classified into subbranks according to the results of detailed investigation. As can be seen, many piers formerly ranked C and D are reassigned the subbranks B1, B2, or B3 which means the main reinforcement needs to be replaced. This is because damage that was presumed to be concrete cracking in the visual inspections was found far more serious in the detailed investigations. For example, buckling of below-ground reinforcement was found by excavation and buckling of main reinforcement within the cover concrete was detected in hammering tests.

4.3 Damage level and damage orientation

Fig. 7 compares damage levels and damage orientation. Approximately half of the damage occurred in both orientations (LT), but the number of damage cases in the direction perpendicular to the bridge axis (T) is greater than that in the bridge axis direction (L). One reason for this is assumed to be that, though the Kobe Route runs in the east-west direction (bridge axis direction), the seismic forces were predominantly in the north-south direction (perpendicular to the bridge axis), and the sustained damage was also predominant in that direction. The other reason is probably that the east-west (axial) direction was more resistant to seismic forces because columns act with girders to resist the forces as compared with the other direction, in which each column resists the forces alone. To verify these assumptions, the results obtained were compared with results from other bridges running in the north-south direction. A considerable difference was found — the majority of damage to these bridges occurred in the direction perpendicular to the bridge axis. This conversely means that in the case of the Kobe Route the direction of seismic forces had an apparent effect. But as the damage level becomes higher, the damage increased in all orientations (LT). This is because the main reinforcement, which buckled first in the direction of the seismic forces expanded out towards the sides as a result of continued seismic loading.

4.4 Shear span ratio and damage type

The piers have shear span ratios ranging from 3 to 7, but approximately 65% of them are in the

range 4 ~ 5. Figure 8 shows the relationship between shear span ratio and damage type. When the shear span ratio is in the range 3 ~ 6, the observed damage is of the shear type, but when the ratio is greater than 7, damage is entirely of the bending type. This is evidence that the shear span ratio also has an effect on damage type.

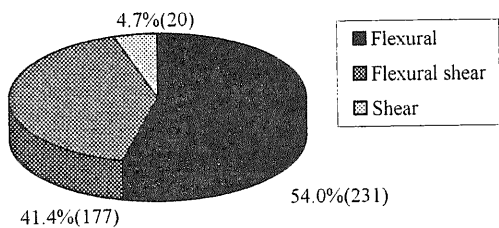


Fig.4 Damage types of RC single piers (all ranks)

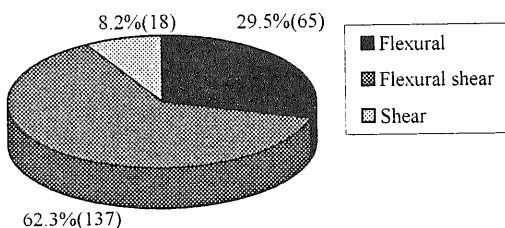


Fig.5 Damage types of RC single piers (As, A, and B ranks)

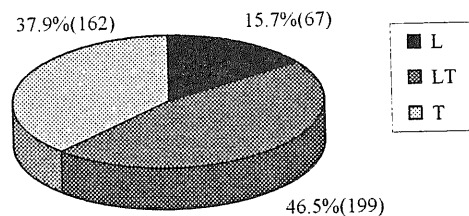


Fig.7 Damage to piers by damage orientation

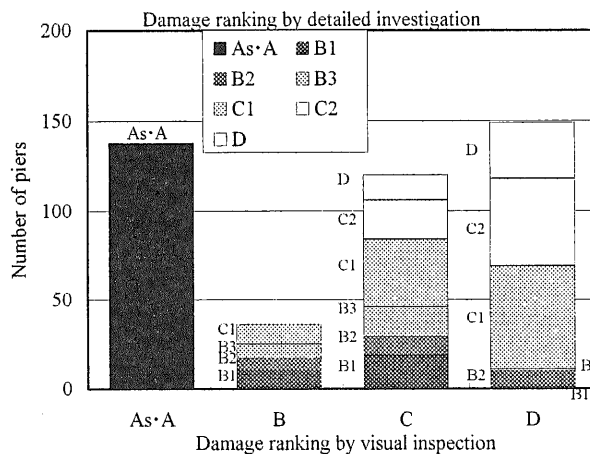


Fig.6 Comparison of damage levels

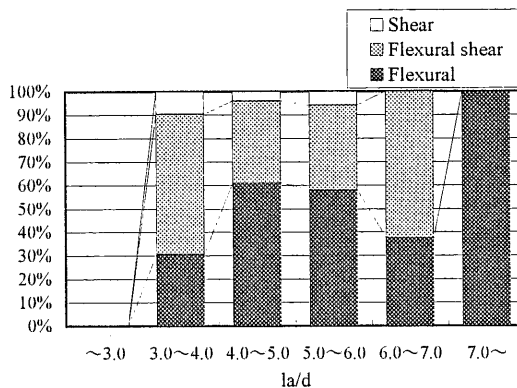


Fig.8 Shear span ratio and damage type

5. ULTIMATE LATERAL STRENGTH AND DAMAGE LEVEL

5.1 Flexural strength and damage level

Figure 9 shows the distribution of safety factors for yield flexural strength for piers that suffered flexural damage. The safety factors are all greater than 1, which means the design value of the then standards is satisfied. The safety factors for yield flexural strength are greater than 1.25 for more than 70% of the piers, so these satisfy the design horizontal seismic coefficient of 0.25 derived by the allowable design method for the Highways Specifications. At higher damage levels, no conspicuous relationships are found between damage level and safety factor for yield

flexural strength (β_{my}), but when the damage level is lower, for example piers of damage ranks C and D, there is a clear relationship between damage level and safety factor for yield flexural strength. This is probably because yield flexural strength has a considerable effect on the damage level at lower damage levels before flexural yielding, but when the damage is serious and exceeds the level of flexural yielding, ductility or the safety factor for shear strength after yielding stage causes a difference in damage level. Figure 10 shows the distribution of safety factors for the ultimate flexural strength of piers that suffered flexural damage. It is clear that, compared with the results in Fig. 9, significant damage of As, A, and B1 ranks occurs less often as safety factor for ultimate flexural strength becomes larger. From this, it can be said that an effective way to minimize damage of flexural type is to secure sufficient ductility.

5.2. Shear strength and damage level

Figure 11 describes the relationship between damage level and safety factor for shear strength in the case of piers of all three damage types. Figure 12 shows a similar relationship for piers that suffered flexural shear damage and shear damage. It is seen from these figures that, as the safety factor for shear strength increases, damage levels tend to fall. The safety factor for shear strength is greater than 1 in all piers, which means the required shear capacity against the design acceleration according to the old standard is satisfied. Over 90% of the piers have a safety factor of greater than 1.25, which means the design acceleration of the current standard is also met. The safety factor for shear strength ranges from 1.0 to 2.5.

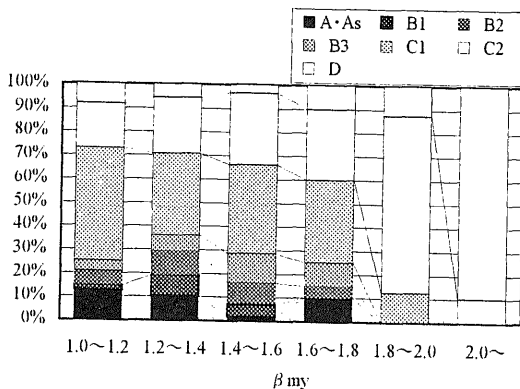


Fig.9 Distribution of safety factor for yielding flexural strength (flexural damage)

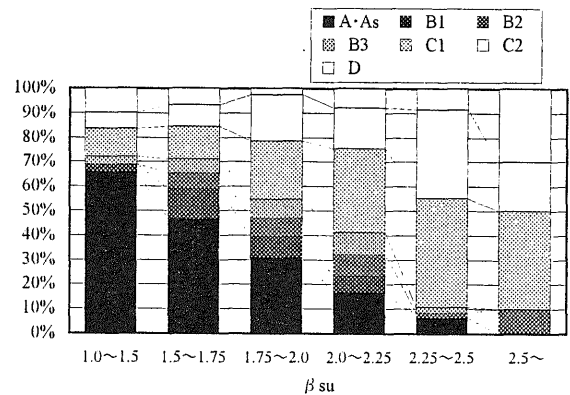


Fig.11 Distribution of safety factor for shear strength (all damage types)

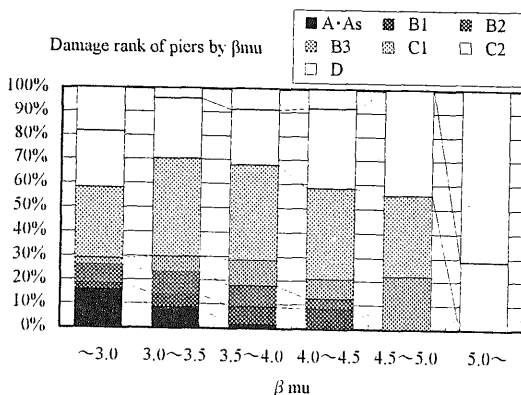


Fig.10 Distribution of safety factor for ultimate flexural strength (flexural damage)

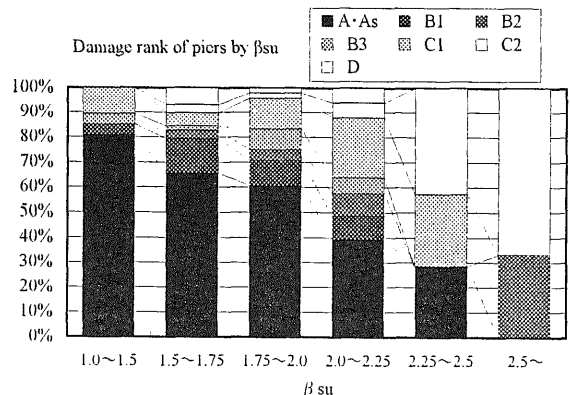


Fig.12 Distribution of safety factor for shear strength (flexural shear and shear damage)

5.3 Discussion of shear strength

Figures 15 and 16 compare the shear strength as specified by the Highway Specifications and the Concrete Specifications. The difference remains slight in the range where both the cross section and the shear strength are relatively small. In contrast, at higher shear strengths, the value given by the Bridge Specifications tends to be 10 ~ 20% larger than that derived from the Concrete Specifications. The difference is attributable to the use of different calculation methods to evaluate the shear strength carried by the concrete. Namely, the method in the Concrete Specifications takes into account the size effect of the cross section. As the cross section becomes larger, the effect of this difference is magnified. In other words, when the cross section is large and the hoop tie ratio is small, the shear strength obtained by the Concrete Specifications falls below that obtained by the Highway Specifications. Piers with greater shear strength tend to have a rectangular cross section. This type of pier is often employed at locations with relatively long spans such as at crossings, or where the cross sectional size of a pier is restricted.

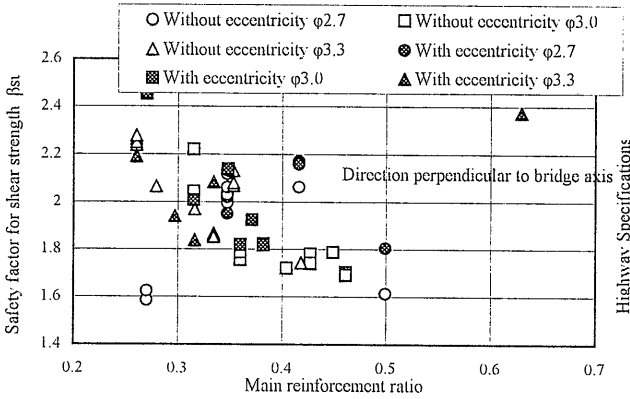


Fig.13 Relationship between safety factor for shear strength and main reinforcement ratio

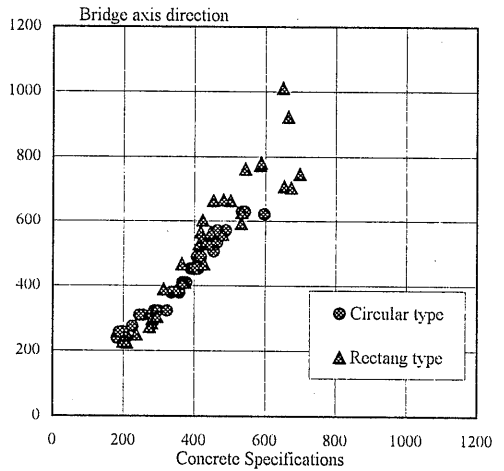


Fig.15 Shear strength by Highway Specifications and Concrete Specifications (bridge axis direction)

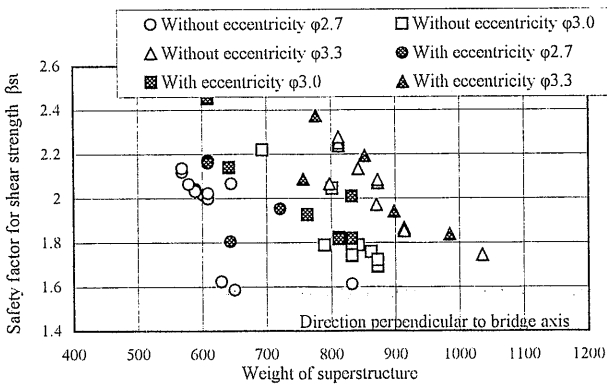


Fig.14 Relationship between safety factor for shear strength and weight of superstructure

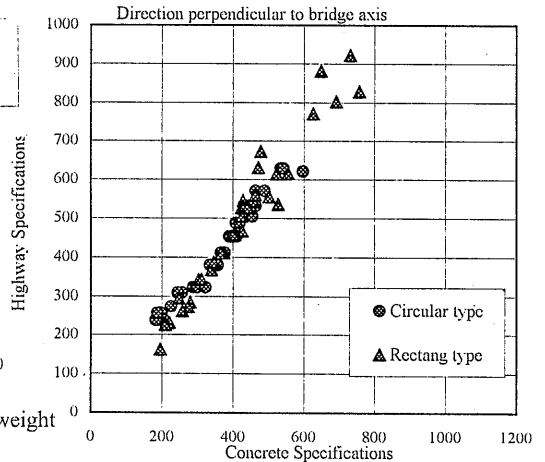


Fig.16 Shear strength by Highway Specifications and Concrete Specifications (direction perpendicular to bridge axis)

6. ANALYSIS OF DAMAGE TYPES

6.1 Shear strength-flexural strength ratio and damage types

Figure 17 presents the relationship between shear strength to flexural strength ratio and damage type (flexural damage and shear damage). Regarding the bending moment, as the actual material strengths of concrete and reinforcing bars are generally 20 ~ 30% larger than the design strength, the ultimate flexural strength is evaluated as 20% higher. As seen from the figure, shear damage is often seen in piers with a small ratio of shear strength to flexural strength. In contrast, flexural damage is observed in piers with a strength ratio of greater than 1. Figure 18 shows the shear strength to flexural strength ratio for piers that suffered flexural shear damage. The strength ratio is distributed in the vicinity of 1, exhibiting no obvious difference from piers that suffered flexural damage.

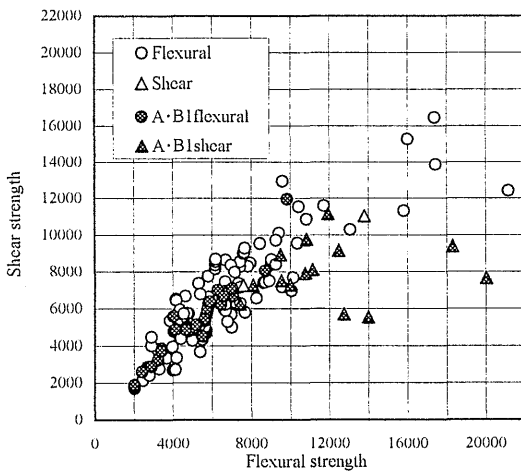


Fig. 17 Shear strength and flexural strength(flexural and shear damage types)

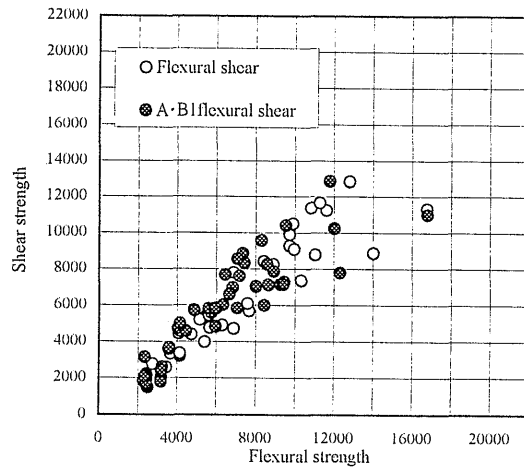


Fig. 18 Shear strength and flexural strength(flexural shear damage types)

6.2 Results for piers with bending damage

Figure 19 shows the relationship between shear strength index (α_{su}) and ultimate flexural strength index (α_{mu}) for piers that suffered flexural damage. It demonstrates that piers of higher damage ranks (B1 and above) are generally those whose α_{su} is lower than 400 gal and α_{mu} lower than 800 gal. Conversely, piers of $\alpha_{su} > 400$ gal and $\alpha_{mu} > 800$ gal are those that had slight damage. It is clear from this that even in piers with flexural damage, the safety factor for shear strength has an effect on the damage level because ductility is a function of shear strength in the range close to the ultimate.

6.3 Results for piers with flexural shear damage

Figure 20 shows the $\alpha_{su} - \alpha_{mu}$ relationship for piers with flexural shear damage. As seen, many of the piers that suffered serious damage have an α_{su} value smaller than 400 gal and α_{mu} smaller than 800 gal, a similar tendency to piers with flexural damage. In particular, piers having an α_{su} value of smaller than 400 gal are mostly those that suffered severe damage. This damage type was caused by a decrease in shear strength as a result of continuing seismic loading after the reinforcement reached flexural yielding.

6.4 Results for piers with shear damage

Figure 21 shows the $\alpha_{su} - \alpha_{mu}$ relationship for piers with shear damage. As compared with piers with flexural damage and flexural shear damage, piers with this damage type had α_{su}

piers with flexural damage and flexural shear damage, piers with this damage type had α_{su} values smaller than 400 gal and they suffered major damage. Thus, shear damage mostly occurred in piers whose shear strength to flexural strength ratio was not more than 1 and with a small safety factor for shear strength.

6.5 Results for piers of all damage types

Table 2 summarizes the overall results. As seen from this table, the damage type can be determined from the shear strength to flexural strength ratio. It is also seen that piers that suffered severe damage has α_{su} values smaller than 400 gal. Flexural damage often occurred in piers with α_{mu} values smaller than 800 gal. Although the piers of the Kobe Route satisfied the allowable stress specified in standards in force at the time they were designed, severe damage occurred to piers where shear fracture occurred first or whose shear strength was reduced by continuing seismic loading. These easily progressed to flexural shear damage.

Now, using Equation (1) given earlier, we can discuss the safety factor required to prevent shear damage. Figure 22 shows the relationship between the shear strength to flexural strength ratio and damage for piers of all damage types. As is clear from the figure, if the shear strength is 1.5 times greater than the flexural strength, flexural damage is most likely to occur. Therefore, to prevent shear damage, it is necessary to introduce a safety factor of greater than 1.5 times the shear strength.

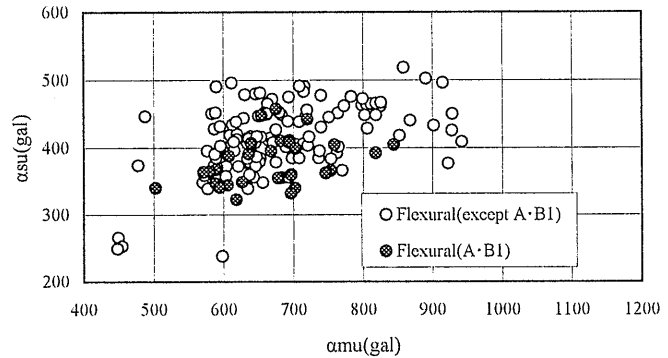


Fig.19 Relationship between shear strength and ultimate lateral strength index (α_{su} - α_{mu} relationship)(flexural damage type)

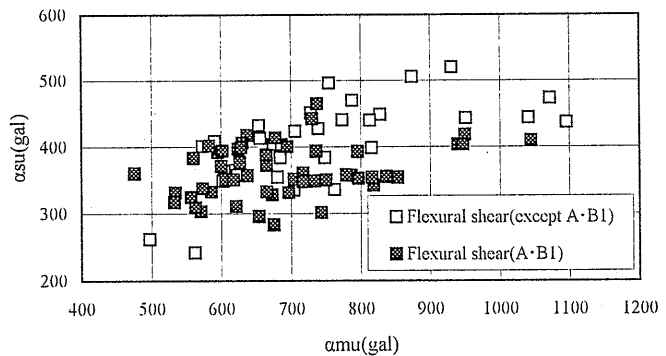


Fig.20 The α_{su} - α_{mu} relationship(flexural shear damage type)

6.6 Ultimate flexural strength index and equivalent natural period

Figure 23 shows the relationship between ultimate flexural strength index and equivalent natural period for piers of all damage types. The yield rigidity of the member was used in calculating the equivalent natural period. As seen from the figure, piers with little damage are very likely to have a large ultimate flexural strength index, and if the moment capacity indices are the same, those piers tend to have a relatively long natural period. Even if the ultimate flexural strength index is large, if the natural period is in the range of approximately 0.5 ~ 0.6 seconds, flexural shear damage of higher rank occurs.

7. REQUIREMENTS FOR SEISMIC STRENGTHENING

From the damage analysis above, the following strengthening measures are recommended to

minimize damage to piers in the event of a strong earthquake.

- ① Increase the shear strength to flexural strength ratio to well above 1 to prevent shear damage.
- ② Provide sufficient shear strength to prevent shear damage and flexural shear damage that may result in significant damage.
- ③ Provide sufficient ductility to minimize flexural damage.

These conclusions indicate that the basic concepts presented in the Seismic Design section of the Highway Specifications and the Concrete Specifications are quite rational. It conversely means that, in the case of piers designed using the old standards, damage attributable to ① and ② is particularly likely because those piers lack sufficient shear strength. Usually, when seismic strengthening is executed, the work has to be prioritized due to constraints such as time and budget. These results clearly indicate that in such a case the highest priority should be given to piers with a small shear strength to flexural strength ratio and a small safety factor for shear strength.

Figure 24 gives the $\alpha_{su} - \alpha_{mu}$ relationship of all three damage types. It is seen that piers having α_{su} and α_{mu} values greater than 450 gal and 800 gal, respectively, suffer a low level of damage in all damage types. Figures 25 and 26 are graphs focusing on the $\alpha_{su} - \alpha_{mu}$ relationship of the four quadrants, A, B, C, and D, sectioned from the graph in Fig. 24. Specifically, Fig. 25 provides a breakdown by damage ranking, and Fig. 26 a breakdown by damage type. It appears from Fig. 25 that the majority of piers in quadrants C and D with α_{su} below 400 gal are those that sustained serious damage (damage of ranks As to B3). Approximately 3/4 of piers in quadrant B with $\alpha_{su} > 400$ and $\alpha_{mu} > 800$ gal suffered relatively light damage (damage of ranks C1, C2, and D). Figure 26 shows that flexural damage is predominant in quadrant A and that shear damage is predominant in quadrant D, indicating that a clear relationship exists between the shear strength to

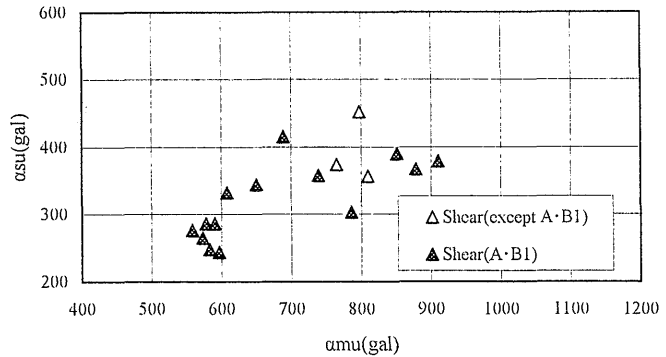


Fig.21 The $\alpha_{su} - \alpha_{mu}$ relationship (shear damage type)

Table 2 Results of assessment

Damage type	Flexural	Flexural shear	Shear
Ratio of shear strength to flexural strength	Mostly greater than 1	Mostly around 1	Mostly smaller than 1
α_{mu} of seriously damaged piers	Mostly smaller than 800 gal	Fairly smaller than 800 gal	Trend unobtainable
α_{su} of seriously damaged piers	More than half smaller than 400 gal	Mostly smaller than 400 gal	Mostly smaller than 400 gal

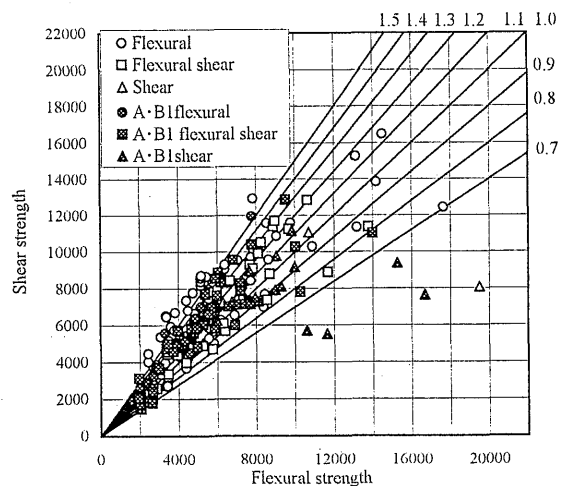


Fig.22 Relationship between shear strength and flexural strength

flexural strength ratio and the type of damage suffered by a pier. It is therefore concluded that piers with sufficient ductility and safety factor for shear strength, in which flexural damage precedes, are able to adequately withstand earthquake loading. These equate to piers in quadrant B.

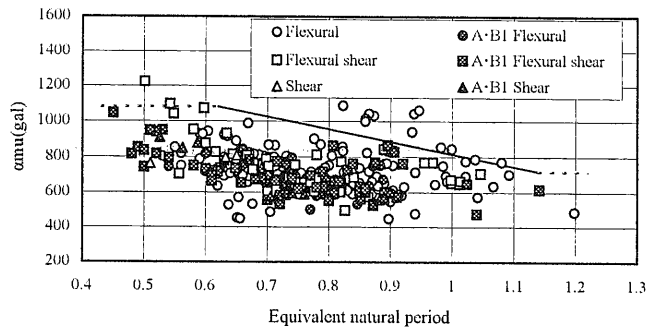


Fig.23 Ultimate flexural strength index and equivalent natural period

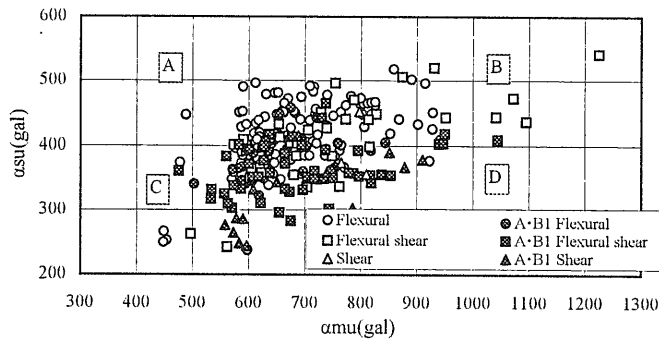


Fig.24 The $\alpha su - \alpha mu$ relationship (all damage types)

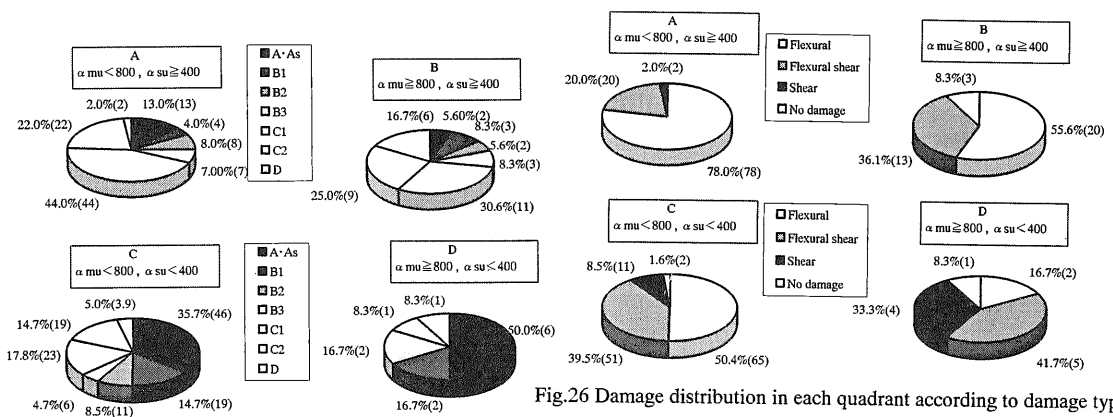


Fig.25 Damage distribution in each quadrant according to rank

Fig.26 Damage distribution in each quadrant according to damage type

8. CONCLUSIONS

Macroscopic damage analysis was conducted on RC single piers along the Hanshin Expressway Kobe Route, which suffered severe damage during the 1995 Hanshin Awaji Earthquake. The focus was on the relationship between damage level and the shear strength to flexural strength ratio, the safety factor for shear strength, and the flexural strength. These characteristics were derived using the seismic ultimate lateral strength method. The following conclusions were drawn from the results:

- ① According to a grouping by damage type, it was found that piers with flexural damage were broadly distributed throughout the damage levels from As to D. In contrast, those that suffered shear damage and flexural shear damage were mostly ranked with damage levels A and B, which mean serious damage. This is because shear damage progresses quite rapidly, and almost never halts at the level of slight damage.
- ② Most damage was found to be in the direction perpendicular to the bridge axis. However, as the level of damage increased, the degree of damage increased in both orientations — in the bridge axis direction and perpendicular to it.
- ③ A correlation was found between damage type — flexural damage, flexural shear damage, or shear damage — and the shear strength to flexural strength ratio. If the strength ratio is smaller than 1, most damage was of shear type. If it is approximately 1, most damage was of flexural shear type.
- ④ A correlation was obtained between damage level and safety factor for shear strength. If piers had a large safety factor, damage was mostly slight. Though all the piers met the design acceleration demands of the standards in force at the time they were designed, a difference was found in safety factor for shear strength depending on the pier shape, superstructure weight, reinforcement arrangement, and amount of eccentricity.
- ⑤ Among piers that suffered flexural damage, seriously damaged piers were mostly those with a small ultimate flexural strength index.
- ⑥ From the above damage analysis, it is concluded that the top priority for seismic strengthening should be piers with a small shear strength to flexural strength ratio and a small safety factor for shear strength. Strengthening design should aim to enhance their shear strength and ductility.

REFERENCES

- [1] Kawashima, K., "Q&A of Hanshin Awaji Earthquake", Concrete Journal, JCI, Vol. 34, No. 5, pp. 76-78, 1996.5 (in Japanese)
- [2] Ishibashi, T., "Damage to Reinforced Concrete Viaducts and Their Design Earthquake Resistance", Concrete Journal, JCI, Vol. 34, No. 11, pp. 56-58, 1996.11 (in Japanese)
- [3] Okamura, H., Saeki, M., Kanatsu, T., Suzuki, M., and Matsumoto, N., "Transition of Seismic Design for Concrete Structures", Proc. of the Symposium on the Hanshin Awaji Earthquake, pp. 563-570, 1996.1 (in Japanese)
- [4] Kawashima, K. and Unjoh, S., "Impact of Hanshin Awaji Earthquake on Seismic Design and Seismic Strengthening on Highway Bridges" Proc. of JSCE, No. 556, I-38, pp. 1-30, 1997.1 (in Japanese)
- [5] Road Association of Japan, "Manual for Earthquake Disaster Countermeasures for Highway Bridges: Post-Earthquake Countermeasures", 1988.2 (in Japanese)
- [6] Hayashi, H. "Retrofit Design of Hanshin Expressway Kobe Route", Doboku-Seko (technical journal), Vol.36, No. 12, pp. 71-76, 1995.11 (in Japanese)
- [7] Road Association of Japan, "Specifications for Highway Bridges: Seismic Design", 1990.5 (in Japanese)
- [8] JSCE, "Standard Specification for Concrete Structures: Design", 1996.6 (in Japanese)
- [9] Committee for Retrofit of Road Bridges Damaged by Hanshin Awaji Earthquake, "Survey Report of Road Bridges Damaged by the Hanshin Awaji Earthquake", 1995.12 (in Japanese)
- [10] Road Association of Japan, "Application of Specifications for Retrofit of Road Bridges Damaged by Hanshin Awaji Earthquake (Draft)", 1995.6 (in Japanese)